SMOS: ESA's Water Mission

Jordi Font[1,3] and Francesc Torres[2,3]

[1]Institut de Ciències del Mar, CSIC, Passeig Marítim 37-49, 08003 Barcelona, Spain, jfont@icm.csic.es
[2]Dept. Teoria del Senyal i Comunicacions, UPC, Jordi Girona s/n, 08034 Barcelona, Spain, xtorres@tsc.upc.edu
[3]SMOS Barcelona Expert Centre, http://www.smos-bec.icm.csic.es

***Abstract* - SMOS (Soil Moisture and Ocean Salinity, European Space Agency) is the first satellite mission addressing the challenge of measuring sea surface salinity and moisture of land from space. It uses an L-band microwave interferometric radiometer with aperture synthesis (MIRAS) that generates brightness temperature images, from which both geophysical variables are derived. This paper presents the principles of operation of the instrument and the algorithmic approach implemented for the retrieval of salinity from MIRAS observations. The retrieval of salinity requires very demanding performances of the instrument in terms of calibration and stability. This text includes material from an article published in the ESA Bulletin in February 2009 [1] and a paper to appear in the Proceedings of IEEE in November 2009 [2]. The latter contains many relevant references not included here.**

***Keywords* - Aperture synthesis, Imaging, Microwave radiometry, Remote sensing, Water cycle**

I. INTRODUCTION

ESA's Water Mission, otherwise known as the Soil Moisture and Ocean Salinity Mission (SMOS) was selected as the second Earth Explorer opportunity mission and launched in November 2, 2009. SMOS single payload, an interferometric microwave radiometer, shall provide global observations of soil moisture and ocean salinity to improve our understanding of the Earth's water cycle.

One of the highest priorities in Earth science and environmental policy issues confronting society today is to understand the potential consequences resulting from modification of the Earth's water cycle due to climate change. The influence of increases in atmospheric greenhouse gases and aerosols on atmospheric water vapour concentrations, clouds, precipitation patterns and water availability must be understood in order to predict the consequences for water availability for consumption and agriculture.

In a warmer climate, increased evaporation may well accelerate the hydrologic cycle, resulting in changes in the patterns of evaporation over the ocean and land and an increase in the amount of moisture circulating through the atmosphere. Many uncertainties remain, however, as illustrated by the inconsistent results given by current numerical weather and climate prediction models regarding the future distribution of precipitation.

It is evident that insufficient data are available today to help improve our scientific knowledge and understanding of the processes influencing the water cycle. Thus, ESA, the French Space Agency (CNES) and Spanish Centre for Development of Industrial Technology CDTI have teamed up to address this key scientific challenge by delivering a fundamentally new satellite tool to realise these new global datasets [3]. The resulting regular, consistent measurement data will be used to improve our understanding of the way in which both the time-varying distribution of soil moisture and ocean salinity regulate the water cycle of our Blue Planet.

Fig. 1. Artist's view of SMOS in orbit (from ESA Medialab)

II. SALINITY DETERMINATION BY MICROWAVE RADIOMETRY AND THE MIRAS INSTRUMENT

Spacecraft remote sensing of Sea Surface Salinity (SSS) [4], using microwave radiometry at low frequencies, was first proposed by Swift and McIntosh, and is now near to be finally demonstrated with SMOS [5]. At L-band the polarized brightness temperature (T_B) measured by a radiometer is linked to salinity in the first centimeter of the ocean through the dielectric constant of sea water. The sensitivity to salinity increases with decreasing frequency (until around 600 MHz), as well as decreases attenuation by the atmosphere (except for heavy rain), and the 1400-1427 MHz window, reserved for passive observations, has advantages for SSS remote sensing. This requires special

care because of the low sensitivity of T_B to SSS: from 0.8 K to 0.2 K per salinity unit, which depends on the ocean temperature, the radiometer incidence angle, and the polarization. It is necessary to separate out the effects on T_B from other parameters such as SST, the impact of ocean roughness, Faraday rotation, etc. The stringent requirements pose technical challenges achieving the required radiometric accuracy and stability. Finally, the low frequency involved requires the use of very large antennas to achieve a moderate spatial resolution on ground. For these reasons, only two L-band space-borne radiometers, until present, have been flown: in 1968 aboard the Cosmos 243 and in 1973 aboard the Skylab S-194.

In 1995, at the "Soil Moisture and Ocean Salinity" Workshop organized at ESTEC (the European Space Research and Technology Centre, Noordwijk, The Netherlands), microwave radiometry at L-band was still considered as the most adequate technique to remotely measure these two geophysical variables. However, instead of the real aperture microwave radiometers that were considered until then, it was concluded that the most promising technique was aperture synthesis radiometry that had successfully been demonstrated a few years earlier. Le Vine *et al.* created in 2000 an SSS map using the Electronically Steered Thinned Array Radiometer (ESTAR), the first 1D synthetic aperture radiometer flown on an aircraft.

Synthetic Aperture Radiometry was developed in the '50s to obtain high resolution radio images of celestial bodies. In 1983, LeVine and Good proposed its use for Earth Observation as a way to increase the angular resolution of individual antennas. As compared to real aperture radiometers, in which T_B maps are obtained by a mechanical scan of a large antenna, in aperture synthesis radiometers [6] a T_B image is formed through Fourier synthesis in a snapshot basis. A synthetic aperture radiometer measures all the cross-correlation products (visibilities [7]) between the polarized signal pairs collected by the array elements, and from them a T_B image is reconstructed through a complex Fourier synthesis process. The total power of the scene is also measured using at least one real aperture radiometer connected to one of the antennas. For simplicity of operation, the array elements are located in a plane.

The most efficient way of sampling the resulting values in the frequency plain is by means of a hexagonal grid. This allows a maximum separation between individual antennas (receivers) equal to the signal wavelength divided by square root of 3 without suffering from aliasing effects in the image reconstruction process. The antenna distribution that allows simultaneously a hexagonal sampling and a maximum spatial coverage is Y-shaped as commonly used in radio astronomy. This configuration was selected for MIRAS (Microwave Interferometric Radiometer with Aperture Synthesis), the instrument on board SMOS. The MIRAS concept was developed at ESA by M. Martín-Neira [8] and consolidated with contribution from UPC.

The image visualised by such a radiometer is a unit circle that includes a field of view (FOV) from -90º to 90º in all directions around boresight. For a radiometer mounted in a satellite the Earth disk and part of the sky will appear in the image. In the case of MIRAS, due to optimisation reasons the antennas separation was augmented until 0.875 wavelengths. This results in that the six closest replicas, generated by the discrete Fourier transform, are overlapped to the basic image and then considerably reducing the alias-free FOV. However, this alias-free area can be extended by introducing the known T_B values that correspond to the image of the sky. The extended alias-free FOV, when represented in the earth reference frame and in SMOS configuration (69 elements in a Y shape, satellite at 755 km high, and the antenna plane tilted 32º) is shown in figure 2.

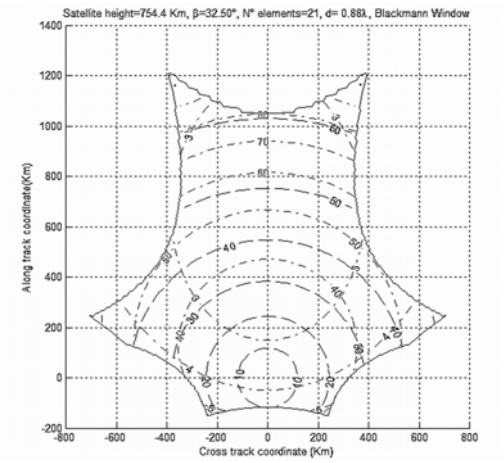

Fig. 2. The SMOS instantaneous alias-free field-of-view (irregular curved hexagon) illustrates the multi-angular and spatially variable nature of the measurements: incidence angle (dashed lines) ranges from 0 to 65º, spatial resolution (dash-dotted lines) from 32 to 100 km, and radiometric sensitivity (dash-dotted) from 2.60 K at boresight to 5 K. As the satellite advances a single spot is seen in successive snapshots under different angles and spatial and radiometric resolutions depending on its position within the instrument field-of-view. Figure generated by the SMOS End-to-end Performance Simulator (UPC).

III. SSS RETRIEVAL WITH SMOS

The basic algorithmic approach selected for SSS retrieval from SMOS radiometric measurements is based on an iterative convergence scheme that compares the measured values with those provided by an L-band forward model of the sea surface emission. This model uses a guessed salinity that can be adjusted until obtaining an optimal fit with the radiometric measurement.

MIRAS allows at each satellite overpass to measure a 2D image of the ocean surface under a wide range of incidence angles, then providing a series of different T_B values corresponding to a single salinity value at a fixed ocean location. This overdetermination is used to reduce the measurement noise and to adjust several geophysical variable parameters that characterize the sea state (for example sea surface temperature, wind speed, significant wave height) and are also included in the forward model,

in addition to SSS, in the iterative minimization process. Besides the low sensitivity of T_B to salinity, three other major problems make the SMOS determination of SSS a real challenge:

1. The instrument limitations (radiometric noise, calibration stability, image reconstruction techniques),
2. The need for precise and simultaneous auxiliary information on the sea surface properties (temperature, roughness, …) to be estimated from external sources, and,
3. The accuracy of the forward model of the sea surface emissivity to be used in the iterative convergence.

The forward model or geophysical model function has to simulate the T_B that reaches the radiometer antenna from the emitting top ocean layer, and this depends on sea water characteristics plus geometry of the ocean surface (roughness), the possibility of other external L-band radiation being backscattered on the roughened surface, and the transformation the overall emission leaving the surface suffers until reaching the antenna.

The L-band emissivity of a flat sea as function of temperature, salinity, viewing angle and polarization is quite well modeled since late 70's, but the different processes that impact on the emission of a roughened surface were not fully described or considered in the several theoretical formulations available at the moment of starting the development of SMOS algorithms. It has been necessary to design and implement several new components of the L-band forward model for the SMOS Level 2 Ocean Salinity Processor (L2OP). This includes a series of tests to sort out in every SMOS snapshot (level 1c data) T_B values that may be wrong due to being contaminated by land or sea ice emission, radio frequency interference, sun and moon glint, or heavy rain attenuation, and several modules to take into account the different effects as explained below.

In a first step, the polarized T_B of the sea can be decomposed in two terms: the "flat sea" contribution (with typical values of 70-150 K depending on the polarization and incidence angle) and a deviation with respect to it that can reach up to 10 K. The deviation term depends on the incidence angle and a parameterization of the surface roughness by means of variables such as wind speed, significant wave height, wave age, atmospheric stability, etc. We can consider that at first order this deviation is independent of SST and SSS, and can be modeled through theoretical formulations (statistical description of the sea surface plus electromagnetic scattering model) or empirical approximations.

The effect of surface roughness is the main geophysical source of error in SMOS salinity retrieval. The changes in the ocean T_B produced by the sea state can be of the same order as the salinity-induced change itself, as the impact of the roughness increase caused by a 10 m/s wind is roughly equivalent to the impact of a modification of SSS by 5 pss at moderate SST. The SMOS L2OP implements three roughness correction model approaches as alternatives to be evaluated and tuned during the mission calibration and validation phase. At present the available data reporting rough sea surface emissivity dependencies with wind speed does not allow to discriminate the best adapted correction between these three models of the roughness impact. All the auxiliary data required for these models will be obtained operationally from the European Centre for Medium range Weather Forecast (ECMWF), and then preprocessed to generate derived variables and to interpolate them at the required spatial and temporal grids.

When high winds generate foam, there is an increase of the T_B, which is function of the sea surface fraction covered by foam and the T_B of the sea foam. Several controlled measurements indicate a foam-induced emissivity in good agreement with the Reul-Chapron model specifically developed for SMOS under some conditions. Other effects that modify sea T_B are those of rain and of oil slicks that can change the sea surface waves spectrum, which affects the T_B. A summary of these effects can be found in.

Before comparing the modeled and measured T_B in the iterative process, it is necessary to add to the sea surface emission the other components of the geophysical model function mentioned above. It is also necessary to geometrically transform the modeled polarized T_B from the Earth reference frame (where the forward model has been applied) to the antenna reference frame (where measurements are done). Several atmospheric effects (upwelling radiation, downwelling radiation scattered over the sea surface, atmospheric/ionospheric losses) are sufficiently well modeled.

The polarization mixing (Faraday rotation), due to the electromagnetic wave propagation through the ionosphere in the presence of the geomagnetic field, can be either modeled from the knowledge of the ionospheric Total Electron Content or avoided by using the first Stokes parameter $I = T_h + T_v$ instead of both polarizations separately in the retrieval. This alternative option presents several other advantages, such as the cancellation of geometric rotation effects when changing the reference basis from surface to antenna planes. It also reduces the uncertainties in the T_B associated to angular dependencies of the sea water dielectric constant model, and in the roughness correction term, even though the number of observables is halved.

Radiation by celestial sources illuminating the ocean surface that are further reflected (through scattering produced by the surface roughness) towards the radiometer has to be taken into account. The T_B of the source brightness, ranging from 2 to 7 K, can be estimated from sky surveys. The surface level scattered signals are computed through a proper weighting of the sky T_B illuminating the considered Earth target by the rough sea surface bistatic scattering coefficients estimated at that point. Reflected solar radiations are extremely intense at L-band (10^5 to 10^7 K) and their contribution needs to be accounted for. With the SMOS orientation, the Sun is present in 97% of the snap-shots. Therefore, Sun cancellation algorithms had to be developed to estimate the T_B coming from the Sun, and subtract it. The few affected grid points and angular measurements will be discarded for salinity retrieval instead of attempting a correction.

The part of the retrieval algorithm that performs the iterative comparison between model and data uses a cost function to be minimized, based on the difference between measured and modeled T_B in the antenna reference frame and incorporating reference values and associated uncertainties, as weights, for the external geophysical parameters (including SSS) that provide information on the sea state conditions, and that will be themselves adjusted during the convergence process. For every pixel on the SMOS FOV, the comparison is made using all available angular measurements acquired in consecutive satellite snapshots. The number of measurements of each pixel depends on the pixel's cross-track distance to the satellite ground-track. As this distance increases, the pixel is imaged fewer times; the angular variation is reduced (Fig. 2) and the instrument's noise increases, which translates into a degraded performance in terms of the quality of the retrieved parameters.

The cost function can also be formulated in terms of the first Stokes parameter (as previously pointed out), or in terms of T_B in the Earth reference frame. However, in this case, in the dual-polarization mode, many pixels have to be discarded since they are affected by large noise amplification in regions close to the singularities of the transformation from the antenna to the Earth reference frames. This situation can be avoided using the full-polarimetric mode, at the cost of larger noise everywhere in the image.

Several of the components described above as steps of the SSS retrieval procedure are specific to the observational approach selected for SMOS, namely aperture synthesis. This technique has a main weakness in the need of performing the complex image reconstruction described in section II and the errors this can introduce. However, it has remarkable strengths compared to measurements made by real aperture antennas. We have highlighted above the multi-angular observation of a single spot that allows taking advantage of the sensitivity of T_B to the incidence angle to increase the robustness of the inversion. Another fundamental feature is the high angular resolution that allows imaging pixels of the order of 30 km and as a consequence identifying different elements within the FOV, like the Sun that can then be removed from the image.

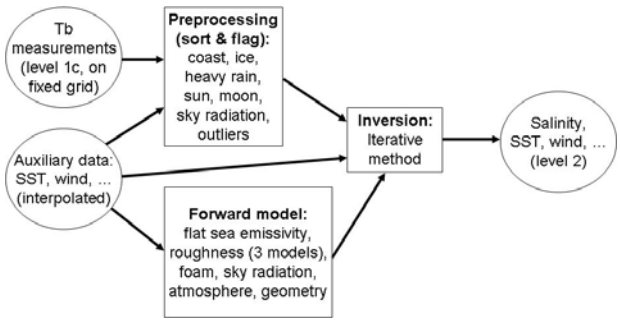

Fig. 3. Diagram of the SMOS salinity retrieval processor

A detailed description of the mentioned different components of the SSS retrieval algorithm (Fig. 3) as they have been implemented in the SMOS L2OP can be found in [9]. The processor was designed for ESA by a team formed by ICM-CSIC, Barcelona (J. Font), Laboratoire d'Océanographie et du Climat—Expérimentation et Approches Numériques (LOCEAN), Paris (J. Boutin) and Institut Français de Recherche pour l'Exploitation de la Mer (IFREMER), Brest (N. Reul).

This paper is a contribution from the SMOS Barcelona Expert Centre on Radiometric Calibration and Ocean Salinity, a joint initiative by Consejo Superior de Investigaciones Científicas (CSIC) and Universitat Politècnica de Catalunya (UPC) established in 2007 and supported by the Spanish National R+D Plan through grant ESP2007-65667-C04. A paper published in 2008 [10] summarises the contributions to SMOS development made by both institutions until

REFERENCES

[1] M. Drinkwater, Y. H. Kerr, J. Font, and M. Berger, "Exploring the water cycle of the blue planet. The Soil Moisture and Ocean Salinity mission," *ESA Bull-Eur Space*, vol. 137, pp. 6-15, 2009.

[2] J. Font, A. Camps, A. Borges, M. Martín-Neira, J. Boutin, N. Reul, Y. H. Kerr, A. Hahne, and S. Mecklenburg, "SMOS: The challenging measurement of sea surface salinity from space," *P. IEEE*, special issue *Satellite Remote Sensing Missions for Monitoring Water, Carbon and Global Climate Change*, in press, 2009.

[3] Y. H. Kerr, P. Waldteufel, J. P. Wigneron, J. M. Martinuzzi, J. Font, and M. Berger, "Soil moisture from space: the Soil Moisture and Ocean Salinity (SMOS) mission," *IEEE T. Geosci. Remote*, vol. 39, pp. 1729-1735, 2001.

[4] G. S. E. Lagerloef, "Satellite Measurements of Salinity," in *Encyclopedia of Ocean Sciences*, J. Steele, S. Thorpe, and K. Turekian, Eds. London: Academic Press, 2001, pp. 2511-2516.

[5] J. Font, G. S. E. Lagerloef, D. M. Le Vine, A. Camps, and O. Z. Zanifé, "The determination of surface salinity with the European SMOS space mission," *IEEE T. Geosci. Remote*, vol. 42, pp. 2196-2205, 2004.

[6] A. Camps, "Application of Interferometric Radiometry to Earth Observation." PhD Thesis: Universitat Politècnica de Catalunya, 1996, 325 pp. (http://www.tdx.cesca.es/TDX-1020104-091741/).

[7] I. Corbella, N. Duffo, M. Vall-llossera, A. Camps, and F. Torres, "The visibility function in interferometric aperture synthesis radiometry," *IEEE Trans. Geosci. Remote*, vol. 42, pp. 1677-1682, 2004.

[8] M. Martín-Neira and J.M. Goutoule, "A two-dimensional aperture-synthesis radiometer for soil moisture and ocean salinity observations," *ESA Bull-Eur Space*, vol. 92, pp 95-104, 1997.

[9] S. Zine, J. Boutin, J. Font, N. Reul, P. Waldteufel, C. Gabarró, J. Tenerelli, F. Petitcolin, J. L. Vergely, M. Talone, and S. Delwart, "Overview of the SMOS sea surface salinity prototype processor," *IEEE T. Geosci. Remote*, vol. 46, pp. 621-645, 2008.

[10] A. Camps, J. Font, M. Vall-Llossera, I. Corbella, N. Duffo, F. Torres, S. Blanch, A. Aguasca, R. Villarino, C. Gabarró, L. Enrique, J. Miranda, R. Sabia, and M. Talone, "Determination of the sea surface emissivity at L-band and application to SMOS salinity retrieval algorithms: Review of the contributions of the UPC-ICM," *Radio Sci.*, vol. 43, Jun 2008.